ELSEVIER

Chemical Engineering Science 62 (2007) 1770–1782

Chemical Engineering Science

www.elsevier.com/locate/ces

Effects of transport and phase equilibrium on fast, nearly irreversible reactive extraction

William B. Zimmerman[a,*], P.O. Mchedlov-Petrossyan[b], G.A. Khomenko[c]

[a]*Department of Chemical and Process Engineering, University of Sheffield, Newcastle Street, Sheffield S1 3JD, UK*
[b]*Institute of Theoretical Physics, NSC Kharkov Institute of Physics and Technology, Ukraine*
[c]*Laboratoire d'Océanografie Côtière du Littoral, ELICO, Université du Littoral Côte d'Opale, MREN, 32, Avenue Foch, 62930, Wimereux, France*

Received 8 November 2005; received in revised form 20 April 2006; accepted 20 April 2006
Available online 29 April 2006

Abstract

Integration of reaction and separation can be exploited to drive reversible reactions in the direction of the desired product using multiphase flow contacting. In the case of nearly irreversible, fast reactions, however, the dynamics of the product have little influence on the reactor efficiency in say liquid–liquid reactive extraction. A similar intensification in reaction efficiency to reactive separation can be achieved by exploiting phase equilibrium or asymmetry in mass transfer rates of the reactants. Here, a model for two-layer biphasic flow and homogeneous reaction is proposed for co-current reactive extraction, demonstrating that localization and intensification of reaction occurs in the region between the entrance and crossover. Crossover occurs if the reactant in stoichiometric deficit preferentially populates the reacting phase due to sufficient imbalance in either mass transfer coefficients or phase equilibrium. We develop an infinite Peclet number (convection dominates over bulk diffusion) model that indicates that crossover occurs when

$$1 > \frac{u_0}{v_0} > \frac{\dfrac{1}{\kappa_{u2}} + \dfrac{1}{\kappa_{u1} h_U}}{\dfrac{1}{\kappa_{v2}} + \dfrac{1}{\kappa_{v1} h_V}}$$

for fast, irreversible reactions. u_0 and v_0 are initial charges to the tubular reactor, the κ's are mass transfer coefficients for each side of the fluid interface and the h's are Henry's Law coefficients for reactants U and V. The interpretation of this formula is that if $v_0 > u_0$, then crossover will occur if the overall mass transfer rate of U is faster than the overall mass transfer rate for V. Downstream of the crossover point, the reactant in stoichiometric excess also dominates the reacting phase due to relative exhaustion of the more-mobile component. A finite Peclet number theory for fast, irreversible reaction shows that the above formula is a conservative limit for crossover—if it holds, crossover will occur regardless of the Peclet number. A formula for the larger parametric region for crossover with finite Peclet number is derived. Verification that crossover is achieved is found by finite-element numerical analysis of the full governing equations. Both theory and numerical analysis predict localization and intensification of the reaction due to crossover. Crossover sets the length scale as approximately two and a half crossover lengths for completed reaction for sufficiently high Peclet number with strong kinetic asymmetry. The theory predicts that taking the ratio of inlet concentrations $S = u_0/v_0$ to be the critical value at fixed physical parameters for mass transfer and phase equilibrium maximizes localization and reactor efficiency. Similarly, the kinetic asymmetry should be as large as possible to exploit the benefits of crossover.

Keywords: Heterogeneous reactions; Mass transfer; Reactive separation; Liquid–liquid reactive extraction; Liquid–liquid equilibria

1. Introduction

Our previous works (Zimmerman et al., 2003; Mchedlov-Petrossyan et al., 2003a,b) show the effect of kinematic

* Corresponding author. Tel.: +44 114 222 7517; fax: +44 114 222 7501.
E-mail address: w.zimmerman@shef.ac.uk (W.B. Zimmerman).

0009-2509/$ - see front matter © 2006 Elsevier Ltd. All rights reserved.
doi:10.1016/j.ces.2006.04.011

asymmetry in fast *heterogeneous* binary reactions where reaction is limited to a *surface of dispersed* phase which could be a solid-supported catalyst particle, droplet, or bubble, on inducing a switch between limiting reagents. Experiments and numerical simulations (Deshpande and Zimmerman, 2005a,b, 2006a,b) also verify that if the stoichiometrically limiting reagent U has a higher mass transfer coefficient, initially it populates the dispersed phase preferentially in a batch reactor, for instance. After a time, the stoichiometrically limiting reagent "catches up" and then it preferentially populates the dispersed phase. This switch from essentially one limiting reagent to the other coincides with a localization in either time (batch) or space (tubular) reactors that is accompanied by an intensification of the reaction. This paper sets out the theory and computes the occurrence of a crossover length in a tubular reactor from reactive extraction from two bulk phases, typically a liquid–liquid system or gas–liquid system. Although the model admits mass transfer rates that are dissimilar, it is shown that the crossover effect occurs when phase equilibrium leads to different partition coefficients in the two phases for the reagents. An irreversible theory, an infinite Peclet number theory, and a finite-element computation of the full mathematical model are presented here, with the prediction of a parametric regime which bounds the crossover phenomenon, and estimates of the localization and intensification of reaction which scale with the crossover length unless the critical surface of the parametric regime for crossover is approached.

1.1. Reactive separation

Reactive separations (see the special edition Gorak (2003)) provide a convenient engineering vehicle for achieving product formation even when the energetics do not favor its formation, i.e. high equilibrium coefficient. It is more than just "two for the price of one", combining both processing steps in one unit operation. It can be used to drive the reaction and thus create reactor efficiency. Reactive extraction has long been used for this purpose, and is used routinely in analytical chemistry (see the review by Bart (2003)) and b ioseparations (Pursell et al., 2003a,b). The advantages of reactive separation are sufficiently large that it should be routinely considered at the flowsheeting stage for process design (Schembecker and Tlatlik, 2003) and in conceptual design (Krishna, 2002). In this paper, we develop a model for reactive extraction which is appropriate for liquid–liquid and gas–liquid contacting. Applications to bioseparations, for instance metabolite separation (Lazarova et al., 2002), are the driver for the flow configuration chosen in Fig. 1. In the laboratory of one of the authors, a microchannel two-phase liquid flow of layers has been set up and controlled. Current state-of-the-art microchannel flows control droplet formation of one phase in the other (Song et al., 2003). Typically, reactive extraction engineers the contacting with dispersed phases so as to maximize the surface area for mass transfer (Prat et al., 2002). In a microfluidic device, however, extensive surface area is already an advantage even of film or layer flows due to the micron scales. Control is the key to successful microfluidic operations. Consequently, the purpose of this paper is to analyze the homogeneous reaction in the upper phase of Fig. 1 to determine whether crossover can be induced in a range of operating parameters, analogous to that for our dispersed phase, heterogeneous reaction models. Undoubtedly it can be from kinetic asymmetry effects alone, so secondarily this paper is targeted to the influence of phase equilibrium on crossover. Furthermore, determining whether there is any advantage to engineering for crossover when phase equilibrium is dissimilar, akin to reactive separation, is an underlying objective. That asymmetry in the phase equilibrium can improve reactor efficiency for irreversible or nearly irreversible fast reactions is examined here. The principle is to control the molecular efficiency by providing the excess reactant *just in time* by phase equilibrium rather than removing the product by phase equilibrium. That this is shown to be the case, even in irreversible reactions, is a novel result unanticipated previously.

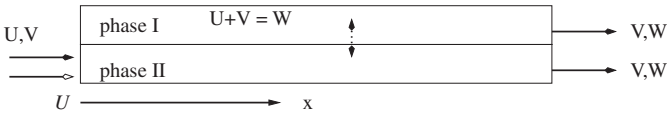

Fig. 1. Idealized tubular reactor for two-phase flow of separated layers with premixed reagents. The reagents enter in phase II, but homogeneous reaction only occurs in phase I. The axial coordinate x corresponds to the direction of the superficial velocity U. Reagent V is stoichiometrically in excess; therefore U is expected to be consumed nearly completely in a finite length of reactor.

1.2. Modeling transport-limited heterogeneous systems

Our recent works have focussed on the dynamics of binary heterogeneous chemical reactions, presuming that the dispersed phase is sufficiently well mixed that at every point in space it is sensible to model the average bulk and surface concentrations of all participating species in the reaction. If the reaction is sufficiently fast, then mass transfer and bulk transport are the controlling mechanisms. In the case of two-layer flow, these mechanisms are present for two bulk phases. Bailey and Ollis (1987) is among the many standard references for the two-film model of mass transfer across the interface, including phase equilibria. In this paper, we augment the interfacial transfer and phase equilibrium with bulk convection and diffusion modeled in the extracting phase and bulk convection, diffusion, and homogeneous reaction in the extracted phase. Standard reaction engineering texts provide the bulk models. See Hill (1977), Levenspiel (1972) and Fogler (1992) for the regime of applicability of the bulk models.

The paper is organized as follows. In Section 2, the governing model equations are presented. In Section 3, two irreversible perturbation theories are presented for finite and infinite Peclet number. The conditions for the occurrence of crossover are derived in each model, and a transcendental equation for the position of crossover is solved numerically. The results are explored in comparison with a full finite-element numerical analysis of the governing equations. An assessment is made for the degree of localization and intensification induced by the existence of crossover. In Section 4, the conclusions are drawn.

2. Modeling axial and interfacial transport

Fig. 1 gives the definition sketch. The salient features are a superficial velocity U which convects the premixed reactants U and V with bulk concentrations u_2 and v_2 in the entry phase and u_1 and v_1 in the reactive phase. The product W, which is generated by reaction in phase I has bulk concentrations w_1 and w_2. There are three interfacial concentrations $\tilde{u}_1$, $\tilde{v}_1$, and $\tilde{w}_1$ on the reactive side of the interface, and three more on the nonreacting side: $\tilde{u}_2$, $\tilde{v}_2$, and $\tilde{w}_2$. The standard bulk conservation equations are

Phase I

$$D\frac{d^2u_1}{dx^2} - U\frac{du_1}{dx} - \xi(u_1v_1 - Kw_1) + \kappa_{u1}(\tilde{u}_1 - u_1) = 0,$$

$$D\frac{d^2v_1}{dx^2} - U\frac{dv_1}{dx} - \xi(u_1v_1 - Kw_1) + \kappa_{v1}(\tilde{v}_1 - v_1) = 0,$$

$$D\frac{d^2w_1}{dx^2} - U\frac{dw_1}{dx} + \xi(u_1v_1 - Kw_1) - \kappa_{w1}(w_1 - \tilde{w}_1) = 0. \tag{1}$$

Phase II

$$D\frac{d^2u_2}{dx^2} - U\frac{du_2}{dx} - \kappa_{u2}(u_2 - \tilde{u}_2) = 0,$$

$$D\frac{d^2v_2}{dx^2} - U\frac{dv_2}{dx} - \kappa_{v2}(v_2 - \tilde{v}_2) = 0,$$

$$D\frac{d^2w_2}{dx^2} - U\frac{dw_2}{dx} + \kappa_{w2}(\tilde{w}_2 - w_2) = 0. \tag{2}$$

The conditions at the interface, assuming pseudo-steady state for mass transfer, are Phase equilibrium, approximated by Henry's Law

$$\tilde{u}_1 = h_U\tilde{u}_2, \quad \tilde{v}_1 = h_V\tilde{v}_2, \quad \tilde{w}_1 = h_W\tilde{w}_2. \tag{3}$$

Stoichiometric constraints on mass transfer:

$$\kappa_{u1}(\tilde{u}_1 - u_1) = \kappa_{u2}(u_2 - \tilde{u}_2),$$

$$\kappa_{v1}(\tilde{v}_1 - v_1) = \kappa_{v2}(v_2 - \tilde{v}_2),$$

$$\kappa_{w1}(w_1 - \tilde{w}_1) = \kappa_{w2}(\tilde{w}_2 - w_2). \tag{4}$$

The boundary conditions are Danckwerts (Bischoff, 1961; Danckwerts, 1953) conditions at the origin and decaying conditions at infinity.

Phase I, Inflow:

$$0 = u_1|_{x\to 0^+} - \frac{D}{U}\frac{du_1}{dx}\bigg|_{x\to 0^+},$$

$$0 = v_1|_{x\to 0^+} - \frac{D}{U}\frac{dv_1}{dx}\bigg|_{x\to 0^+},$$

$$0 = w_1|_{x\to 0^+} - \frac{D}{U}\frac{dw_1}{dx}\bigg|_{x\to 0^+}. \tag{5}$$

Phase I, Outflow:

$$\frac{du_1}{dx}\bigg|_{x\to\infty} = \frac{dv_1}{dx}\bigg|_{x\to\infty} = \frac{dw_1}{dx}\bigg|_{x\to\infty} = 0. \tag{6}$$

Phase II, Inflow:

$$u_0 = u_2|_{x\to 0^+} - \frac{D}{U}\frac{du_2}{dx}\bigg|_{x\to 0^+},$$

$$v_0 = v_2|_{x\to 0^+} - \frac{D}{U}\frac{dv_2}{dx}\bigg|_{x\to 0^+},$$

$$0 = w_2|_{x\to 0^+} - \frac{D}{U}\frac{dw_2}{dx}\bigg|_{x\to 0^+}. \tag{7}$$

Phase II, Outflow:

$$\frac{du_2}{dx}\bigg|_{x\to\infty} = \frac{dv_2}{dx}\bigg|_{x\to\infty} = \frac{dw_2}{dx}\bigg|_{x\to\infty} = 0. \tag{8}$$

2.1. Scaling and dimensional analysis

Since the overall process is taken to be mass transfer limited, we select the characteristic time as $\tau = \kappa_{v1}^{-1}$. The characteristic time for the homogeneous reaction in phase I is ξ^{-1}. We introduce a parameter ε as the ratio of these two time scales:

$$\varepsilon = \frac{\kappa_{v1}}{\xi}, \tag{9}$$

with the assumption of fast reaction, $\varepsilon \ll 1$. As a length scale, we introduce a "convective mass transfer length", i.e. the length $L = U\tau = U/\kappa_{v1}$ in which the superficial velocity convects a tracer element in the unit mass transfer time. The dimensionless parameter that arises for the relative importance of convection to diffusion is a "quasi-Peclet number," $p = UL/D$. Scaling the nondimensional coordinate by L gives $z = x/L$. The other dimensionless groups that arise naturally are ratios of mass transfer coefficients:

$$\nu_{u1} = \frac{\kappa_{u1}}{\kappa_{v1}}, \quad \nu_{w1} = \frac{\kappa_{w1}}{\kappa_{v1}}, \quad \nu_{u2} = \frac{\kappa_{u2}}{\kappa_{v1}}, \quad \nu_{v2} = \frac{\kappa_{v2}}{\kappa_{v1}},$$

$$\nu_{w2} = \frac{\kappa_{w2}}{\kappa_{v1}}. \tag{10}$$

The partition coefficients for the three Henry's Law phase-equilibrium constraints and the reaction equilibrium constant are already dimensionless. With these scalings and parameters, the dimensionless equations now take the form:

$$\frac{1}{p}\frac{d^2u_1}{dz^2} - \frac{du_1}{dz} - \frac{1}{\varepsilon}(u_1v_1 - Kw_1) + \nu_{u1}(\tilde{u}_1 - u_1) = 0,$$

$$\frac{1}{p}\frac{d^2v_1}{dx^2} - \frac{dv_1}{dx} - \frac{1}{\varepsilon}(u_1v_1 - Kw_1) + (\tilde{v}_1 - v_1) = 0,$$

$$\frac{1}{p}\frac{d^2w_1}{dx^2} - \frac{dw_1}{dx} - \frac{1}{\varepsilon}(u_1v_1 - Kw_1) - \nu_{w1}(w_1 - \tilde{w}_1) = 0. \tag{11}$$

$$\frac{1}{p}\frac{\mathrm{d}^2u_2}{\mathrm{d}z^2}-\frac{\mathrm{d}u_2}{\mathrm{d}z}-v_{u2}(u_2-\tilde{u}_2)=0,$$

$$\frac{1}{p}\frac{\mathrm{d}^2v_2}{\mathrm{d}x^2}-\frac{\mathrm{d}v_2}{\mathrm{d}x}-v_{v2}(v_2-\tilde{v}_2)=0,$$

$$\frac{1}{p}\frac{\mathrm{d}^2w_2}{\mathrm{d}x^2}-\frac{\mathrm{d}w_2}{\mathrm{d}x}+v_{w2}(\tilde{w}_2-w_2)=0. \tag{12}$$

Eq. (3) still holds for the phase-equilibrium constraints. The scaled mass transfer constraints are

$$v_{u1}(\tilde{u}_1-u_1)=v_{u2}(u_2-\tilde{u}_2),$$

$$(\tilde{v}_1-v_1)=v_{v2}(v_2-\tilde{v}_2),$$

$$v_{w1}(w_1-\tilde{w}_1)=v_{w2}(\tilde{w}_2-w_2). \tag{13}$$

The boundary conditions are now:

$$0=u_1|_{z\to0^+}-\frac{1}{p}\frac{\mathrm{d}u_1}{\mathrm{d}z}\bigg|_{z\to0^+},$$

$$0=v_1|_{z\to0^+}-\frac{1}{p}\frac{\mathrm{d}v_1}{\mathrm{d}z}\bigg|_{z\to0^+},$$

$$0=w_1|_{z\to0^+}-\frac{1}{p}\frac{\mathrm{d}w_1}{\mathrm{d}z}\bigg|_{z\to0^+}. \tag{14}$$

$$\frac{\mathrm{d}u_1}{\mathrm{d}z}\bigg|_{z\to\infty}=\frac{\mathrm{d}v_1}{\mathrm{d}z}\bigg|_{z\to\infty}=\frac{\mathrm{d}w_1}{\mathrm{d}z}\bigg|_{z\to\infty}=0. \tag{15}$$

$$u_0=u_2|_{z\to0^+}-\frac{1}{p}\frac{\mathrm{d}u_2}{\mathrm{d}z}\bigg|_{z\to0^+},$$

$$v_0=v_2|_{z\to0^+}-\frac{1}{p}\frac{\mathrm{d}v_2}{\mathrm{d}z}\bigg|_{z\to0^+},$$

$$0=w_2|_{z\to0^+}-\frac{1}{p}\frac{\mathrm{d}w_2}{\mathrm{d}z}\bigg|_{z\to0^+}. \tag{16}$$

$$\frac{\mathrm{d}u_2}{\mathrm{d}z}\bigg|_{z\to\infty}=\frac{\mathrm{d}v_2}{\mathrm{d}z}\bigg|_{z\to\infty}=\frac{\mathrm{d}w_2}{\mathrm{d}z}\bigg|_{z\to\infty}=0. \tag{17}$$

3. Theory for irreversible reaction

Most industrial processes are designed with operating conditions that heavily favor product formation. There are only two ways to accomplish this: (i) the reaction temperature is adjusted so that the equilibrium constant is driven sufficiently low, $K \ll 1$; (ii) separation of the product occurs simultaneously with reaction, usually driven by phase equilibrium rejecting the product from the reacting phase. In this flow configuration, parametric values can be selected so that either mechanism is applicable. The former case is usually achievable with extreme temperatures. The latter requires $h_W \ll 1$ so that the nonreacting phase carries the product away preferentially. If the product is more mobile than the reactants, i.e. $v_{w1} \gg v_{u1}, 1$ and $v_{w2} \gg v_{u2}, v_{v2}$, this alone is not sufficient to remove the product rapidly unless the product can disperse away in the nonreacting phase due to high gradients. Fig. 1 defines a co-current contactor for reactive extraction that is typically poorer than countercurrent contactors in maintaining high gradients in the extracted species (the product).

Here we present two approximate theories for high Peclet number operation. Generally, since diffusion is such a weak process, even in laminar flow high Peclet number operation is common. For turbulent flow, even with stronger dispersive mixing leading to higher effective diffusivity coefficients, superficial velocities are typically sufficiently strong to ensure high Peclet number operation. Thus, it is certainly practically useful to develop a high Peclet number theory. The irreversible asymptotic equations are presented in Section 3.1 and analyzed in Section 3.2. Since the reaction kinetics simplify in the irreversible limit to piecewise linear with either one reactant or the other vanishing, it is possible to write solutions in closed form for all eight reactant concentrations.

3.1. Irreversible equations

Strictly irreversible reaction simplifies Eqs. (11)–(17) in two ways. First, the dynamics of the product decouple from those of the reactants. Secondly, for a fast reaction one or the other (or even both) reactant concentrations vanish in the reactive phase (phase I). The differential constraints take the form:

Phase I

$$\varepsilon\left[\frac{1}{p}\frac{\mathrm{d}^2u_1}{\mathrm{d}z^2}-\frac{\mathrm{d}u_1}{\mathrm{d}z}+v_{u1}(\tilde{u}_1-u_1)\right]-u_1v_1=0,$$

$$\varepsilon\left[\frac{1}{p}\frac{\mathrm{d}^2v_1}{\mathrm{d}z^2}-\frac{\mathrm{d}v_1}{\mathrm{d}z}+(\tilde{v}_1-v_1)\right]-u_1v_1=0, \tag{18}$$

$$\frac{1}{p}\frac{\mathrm{d}^2u_2}{\mathrm{d}z^2}-\frac{\mathrm{d}u_2}{\mathrm{d}z}+v_{u2}(\tilde{u}_2-u_2)=0,$$

$$\frac{1}{p}\frac{\mathrm{d}^2v_2}{\mathrm{d}z^2}-\frac{\mathrm{d}v_2}{\mathrm{d}z}+v_{v2}(\tilde{v}_2-v_2)=0. \tag{19}$$

The first two of the Henry's Law constraints (3) and the first two stoichiometric constraints on the mass transfer flux (13) continue to hold without change of form and are pertinent here. These four constraints may be considered as a system of equations to determine the equilibrium concentrations in terms of bulk concentrations as follows:

$$\tilde{u}_1=h_U\frac{u_1+v_{u2}u_2}{h_Uv_{u1}+v_{u2}},\quad \tilde{u}_2=\frac{u_1+v_{u2}u_2}{h_Uv_{u1}+v_{u2}}, \tag{20}$$

$$\tilde{v}_1=h_V\frac{v_1+v_{v2}v_2}{h_V+v_{v2}},\quad \tilde{v}_2=\frac{v_1+v_{v2}v_2}{h_V+v_{v2}}. \tag{21}$$

Substituting Eqs. (20) and (21) into the conservation equations (18) and (19), we reformulate the problem in terms of bulk concentrations only.

$$\frac{1}{p}\frac{\mathrm{d}^2u_1}{\mathrm{d}z^2}-\frac{\mathrm{d}u_1}{\mathrm{d}z}+v_{u1}v_{u2}\frac{h_Uu_2-u_1}{h_Uv_{u1}+v_{u2}}-\frac{1}{\varepsilon}u_1v_1=0, \tag{22}$$

$$\frac{1}{p}\frac{\mathrm{d}^2v_1}{\mathrm{d}z^2}-\frac{\mathrm{d}v_1}{\mathrm{d}z}+v_{v2}\frac{h_Vv_2-v_1}{h_V+v_{v2}}-\frac{1}{\varepsilon}u_1v_1=0, \tag{23}$$

$$\frac{1}{p}\frac{d^2u_2}{dz^2} - \frac{du_2}{dz} - v_{u1}v_{u2}\frac{h_U u_2 - u_1}{h_U v_{u1} + v_{v2}} = 0, \tag{24}$$

$$\frac{1}{p}\frac{d^2v_2}{dz^2} - \frac{dv_2}{dz} - v_{v2}\frac{h_V v_2 - v_1}{h_V + v_{v2}} = 0. \tag{25}$$

Combining Eqs. (22)–(25) we get

$$\frac{1}{p}\frac{d^2}{dz^2}(u_1 + u_2 - v_1 - v_2) - \frac{d}{dz}(u_1 + u_2 - v_1 - v_2) = 0. \tag{26}$$

The only nonincreasing solution for this equation is a constant, which can be fixed from the inlet conditions at $z = 0$ to obtain

$$u_1 + u_2 - v_1 - v_2 = u_0 - v_0. \tag{27}$$

Two linear differential constraints (24), (25), the algebraic constraint (27) and one of nonlinear differential constraints (22) or (23) constitute the complete system of four equations for unknowns u_1, u_2, v_1 and v_2.

3.2. Finite Peclet number, fast-reaction asymptotic theory

If neither the Peclet number p is too small, nor the mass transfer coefficients differ too much in different phases ($v_{u1} \sim O(1)$), then a regular perturbation approximation for fast reaction, small $\varepsilon \ll 1$ but nonvanishing, is well posed. We look for solutions of the form

$$u_1 = u_1^{(0)} + \varepsilon u_1^{(1)} + O(\varepsilon^2), \quad v_1 = v_1^{(0)} + \varepsilon v_1^{(1)} + O(\varepsilon^2), \tag{28}$$

$$u_2 = u_2^{(0)} + \varepsilon u_2^{(1)} + O(\varepsilon^2), \quad v_2 = v_2^{(0)} + \varepsilon v_2^{(1)} + O(\varepsilon^2). \tag{29}$$

The homogeneous reactive flux simplifies as well to first order in ε as

$$u_1 v_1 = u_1^{(0)} v_1^{(0)} + \varepsilon\left(u_1^{(0)} v_1^{(1)} + v_1^{(0)} u_1^{(1)}\right) + O(\varepsilon^2). \tag{30}$$

To leading order in ε, the equations for the reactive phase (phase I) undergo a massive simplification:

$$u_1^{(0)} v_1^{(0)} = 0. \tag{31}$$

Eqs. (24) and (25) for phase II, as well as the conservation law (27) are linear and therefore have the same form for all orders in ε. The system of equation thus obtained may be solved by the procedure quite similar to one used in Mchedlov-Petrossyan et al. (2003b). Although cumbersome, these solutions can be used to pose the question of the existence of a crossover point in the reactive phase—from nearly depleted of the reactant in stoichiometric excess to nearly depleted of the stoichiometrically limiting reactant. Intuitively, this could occur if the limiting reactant is either more mobile or preferentially occupies the reactive phase due to phase equilibria. In Section 3.2, we explore the parametric interplay of stoichiometry and phase equilibrium on the existence and position of crossover. The constraint on crossover does not lend itself to analytic solution, since the equation is transcendental, so numerical computations of the solutions are compared with full finite-element solutions to the reversible kinetics of Eqs. (11)–(17) with estimates of the crossover length X. Since crossover is only defined uniquely by the $K = 0$ theory, the analogous value for reversible kinetics is open to interpretation. Here, for our finite-element simulations, two plausible definitions are put forth, though resulting in similar values and trends. The one adopted for presentation is the $z = X$ such that $u_1^{(0)} = v_1^{(0)}$—the concentration values cross.

3.2.1. Initial region asymptotic solution

It follows from Eq. (31) that either $u_1^{(0)}$ or $v_1^{(0)}$, or both are equal to zero. Since the boundary conditions for both reactants in the reactive phase are homogeneous, there is no a priori selection for $u_1^{(0)}$ or $v_1^{(0)}$. We assume first the case that $v_1^{(0)} = 0$ at the reactor inlet and that this case persists for at least some spatial extent downstream, while generally $u_1^{(0)} \neq 0$. This case would occur if preference is given to V populating the reactive phase. It is the more volatile component in the suggested gas–liquid scenario of Fig. 1 or with no phase equilibrium selection, then V is the kinetically faster species at passing the phase barrier. There are analogues in liquid–liquid reactive extraction and in selectively permeable membranes.

By applying this assumption to Eqs. (24), (25) and (27),

$$\frac{1}{p}\frac{d^2u_2^{(0)}}{dz^2} - \frac{du_2^{(0)}}{dz} - v_{u1}v_{u2}\frac{h_U u_2^{(0)} - u_1^{(0)}}{h_U v_{u1} + v_{u2}} = 0, \tag{32}$$

$$\frac{1}{p}\frac{d^2v_2^{(0)}}{dz^2} - \frac{dv_2^{(0)}}{dz} - v_{v2}\frac{h_V v_2^{(0)}}{h_V + v_{v2}} = 0, \tag{33}$$

$$u_1^{(0)} + u_2^{(0)} - v_2^{(0)} = u_0 - v_0. \tag{34}$$

Eliminating $u_1^{(0)}$ from Eqs. (32) and (34) we obtain

$$\frac{1}{p}\frac{d^2u_2^{(0)}}{dz^2} - \frac{du_2^{(0)}}{dz} - \frac{v_{u1}v_{u2}(h_U + 1)}{h_U v_{u1} + v_{u2}}u_2^{(0)} + \frac{v_{u1}v_{u2}}{h_U v_{u1} + v_{u2}}\left(u_0 - v_0 + v_2^{(0)}\right) = 0. \tag{35}$$

The former of these equations is a homogeneous linear second-order differential equation with constant coefficients, whose solution is found by characteristic equations for the exponential decay rate(s). Here it can be shown that at most one of the characteristics yields decay with positive z. If the local deficit of V persists for all z only decaying exponential should be taken. Application of the inlet conditions gives

$$v_2^{(0)} = \frac{v_0 p}{p + \beta_2}\exp(-\beta_2 z),$$
$$\beta_2 = -\frac{p}{2} + \sqrt{\frac{p^2}{4} + \frac{p h_V v_{u2}}{h_V + v_{u2}}}. \tag{36}$$

The second equation of (36) is an inhomogeneous linear second-order ODE with constant coefficients and can be solved for the general homogeneous solution from its characteristic polynomial and for the particular solution by the method of undetermined coefficients. Again, only nonincreasing solution

should be taken, with the increment

$$-\gamma_2 = \frac{p}{2} - \sqrt{\frac{p^2}{4} + \frac{p v_{u1} v_{u2}(1+h_V)}{v_{u2} h_U + v_{u2}}}. \tag{37}$$

3.2.2. Asymptotic solution after a crossover point

The above solution could persist for all time if only $v_2^{(0)}$ is considered—monotonic decay to zero. However, the other two dynamically active concentrations $u_2^{(0)}$ and $u_1^{(0)}$, are not constrained by the equations to be positive definite. In particular, some value of $z = X$ may exist for which $u_1^{(0)} = 0$. This co-vanishing point still satisfies the original assumptions, but downstream of this point, negative $u_1^{(0)}$ is nonphysical, so there is a transition to a second case, with $u_1^{(0)} = 0$ thereafter and generally $v_1^{(0)} \neq 0$ and building up since it is the reactant in overall stoichiometric excess ($v_0 > u_0$) for there to be any logical opportunity for such a transition to occur. The condition for the existence of a crossover point X is independent of the solution in the region after the crossover point. The analytic solution for the concentration profiles downstream of X is analogous to that above. It cannot be found simply from interchanging the symbols u and v, however, since the governing system is not fully symmetrical in our dimensionless scaling, and the boundary conditions apply at $z = X$ for the nonreacting phase from the initial solution. The solution is too complex to show but is straightforward, though tedious. Both the initial and final region solutions were coded in a symbolic solver (Mathematica). They rely on the solution of a transcendental equation for X for their regime of applicability.

3.3. Asymptotic solution for the crossover point

The condition $u_1^{(0)} = 0$ is in general the difference of two exponentials with a constant, which can potentially be satisfied if the negative contribution decays slower than the positive one. Since our target is to understand the primary influence of phase equilibrium on the existence of crossover, we consider only the simplified case of $v_{u1} = v_{u2} = v_{v2} = 1$, $h_U = 1$, $h_V = h$ and $u_0 = S$, $v_0 = 1$, so that the three parameters explored are h, S, and p. With this parametric simplification, the condition for crossover is

$$0 = f_1(h, S, p) + f_2(h, S, p)\exp(-\beta_2 X) + f_3(h, S, p)\exp(-\beta_4 X), \tag{38}$$

where

$$\beta_4 = -\frac{p}{2} + \sqrt{p + \frac{p^2}{4}},$$

and

$$f_1 = (S-1)\left(\sqrt{p} + \sqrt{p+4}\right)\left(\sqrt{p} + \sqrt{\frac{p + h(4+p)}{h+1}}\right),$$

$$f_2 = -2(h-1)\left(p + \sqrt{p^2 + 4p}\right),$$

$$f_3 = 2(h-S)\left(p + \sqrt{\frac{p^2 + hp(4+p)}{h+1}}\right). \tag{39}$$

It should be noted that we originally solved for $u_1^{(0)}$ by retaining the increasing mode $c_2\exp(\beta_3 z)$, where

$$\beta_3 = \frac{p}{2} + \sqrt{p + \frac{p^2}{4}}$$

in the initial region before crossover. Since this mode does not extend to $z \to \infty$ if there is a crossover point, it is not disallowed by the condition of regularity at infinity. The upshot is that to consistently pose conditions for the unknown coefficient c_2, we need to solve for the solution downstream of the crossover point, apply boundary conditions at infinity and at $z = X$, which then completely specify c_2. The constraint on X is far less concise than Eq. (39), yet the resultant numerical solutions by Newton–Raphson root finding found $c_2 \sim O(10^{-15})$ with double precision arithmetic for all parametric values tested. So the shortcut approach of rejecting all modes growing at infinity admits the approximation (39) to an extremely high level of accuracy.

Whether or not a crossover point exists simply depends on the initial slope of the RHS of Eq. (38). If it is an initially increasing function of z, then a crossover point must eventually occur. By setting this initial slope to zero, we find the condition of criticality among h, S, p:

$$0 = -p\left(\sqrt{p+4} - \sqrt{\frac{p+h(4+p)}{h+1}}\right)(2h - 1 - S) + (S-1)\left[\sqrt{p+4}\sqrt{\frac{p^2 + hp(4+p)}{h+1}} - p^{3/2}\right]. \tag{40}$$

This relationship is linear in S and quadratic in h, so it is especially easy to interpret the critical S, for instance, for fixed h and p as a design criteria:

$$S_{\text{crit}} = \frac{-p + \sqrt{4+p}\sqrt{\frac{p+h(4+p)}{1+h}} + (-1+2h)\sqrt{p}\left(\sqrt{4+p} - \sqrt{\frac{p+h(4+p)}{1+h}}\right)}{(-\sqrt{p} + \sqrt{4+p})\left(\sqrt{p} + \sqrt{\frac{p+h(4+p)}{1+h}}\right)}. \tag{41}$$

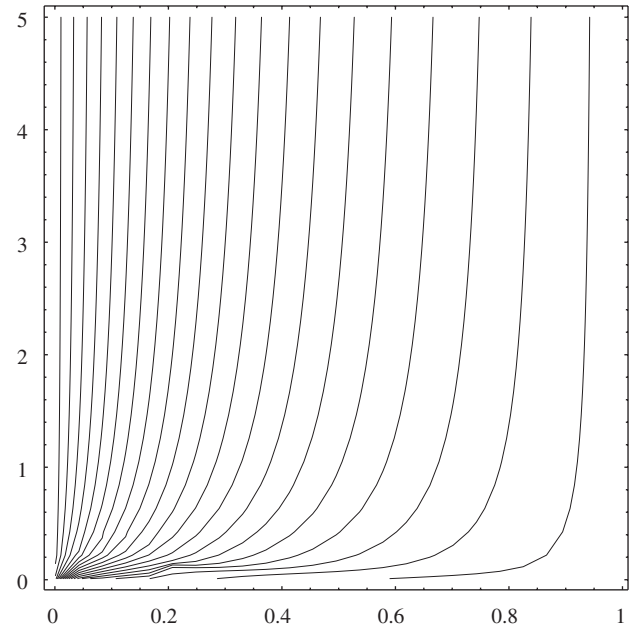

Fig. 2. Contours of critical stoichiometric ratio S_{crit} with variations of p (vertical coordinate) and $h_V = h$ (horizontal coordinate) at fixed unit mass transfer ratios and $h_U = 1$ with *irreversible*, *fast* reaction kinetics. This graph shows high Peclet number near invariance of S_{crit} and a collapse of all contours onto the origin, i.e. only perfect phase selection gives crossover with no convection.

Fig. 2 shows the contours of S_{crit} computed from Eq. (41). They are computed with variations of p (vertical coordinate) and $h_V = h$ (horizontal coordinate) at fixed unit mass transfer ratios and $h_U = 1$ with *irreversible*, *fast* reaction kinetics. This graph shows high Peclet number near invariance of S_{crit} and a collapse of all contours onto the origin, i.e. only perfect phase selection gives crossover with no convection. This latter point suggests that a high Peclet number theory would be simpler and widely applicable.

3.4. Infinite Peclet number theory bounding the crossover regime

In theory, if $p \to \infty$ is a regular limit point of the system, we can compute all quantities from limits of the finite Peclet number theory presented in the last subsection. Potentially, $p \to \infty$ could be a singular limit since $1/p$ multiplies the highest derivative term. Thus a boundary condition must be forfeited in applying the infinite Peclet theory. High but finite Peclet numbers could have a boundary layer that makes the quality of the infinite Peclet solution structurally different. In practice, however, the rejection of all growing-at-infinity modes in the finite Peclet number theory selects the same structural components of the solution as the infinite Peclet theory, and thus regularity is achieved. The analysis completely follows that of the previous argument, but is simpler symbolically.

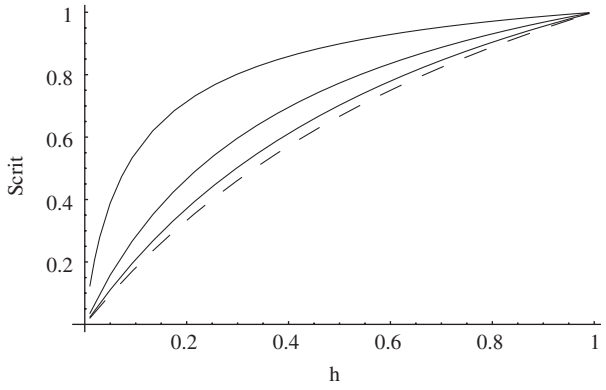

Fig. 3. Curves of critical stoichiometric ratio S_{crit} on the vertical coordinate with variations of p=0.1, 1, 5 (solid lines) and h_V=h (horizontal coordinate) at fixed unit mass transfer ratios and $h_U = 1$ with *irreversible*, *fast* reaction kinetics. The dashed line represents the infinite Peclet number theory with $S_{\text{crit}} = 2h/(1+h)$. This graph shows high Peclet number near invariance of S_{crit} and that the infinite Peclet number critical region is always contained within the finite Peclet number supercritical region. Thus, at given h, designing for operation with $S = 2h/(1+h)$ will result in crossover, regardless of the Peclet number.

The constraint on X takes the form

$$0 = (h-1)\exp(X) + (h-S)\exp\left(\frac{hX}{1+h}\right) + (S-1)\exp\left(X + \frac{hX}{1+h}\right). \tag{42}$$

This is still a transcendental equation, but not as complicated as Eq. (38). The condition for criticality is even simpler yet:

$$S_{\text{crit}} = \frac{2h}{1+h}. \tag{43}$$

Fig. 3 shows graphically that the critical S curves approach this limiting curve even for very low Peclet numbers, say $p = 5$, as suggested by the high Peclet number near vertical slope of the contours in Fig. 2. This graph shows high Peclet number near invariance of S_{crit} and that the infinite Peclet number critical region is always contained within the finite Peclet number supercritical region. Thus, at given h, designing for operation with $S = 2h/(1+h)$ will result in crossover, regardless of the Peclet number.

Even with full parametric variation for mass transfer, the criticality condition that the slope of $u_1^{(0)}$ increases at the origin still takes a simple form. It is more suggestive in dimensional form that crossover occurs if and only if

$$1 > \frac{u_0}{v_0} > \frac{\dfrac{1}{\kappa_{u2}} + \dfrac{1}{\kappa_{u1}h_U}}{\dfrac{1}{\kappa_{v2}} + \dfrac{1}{\kappa_{v1}h_V}}. \tag{44}$$

On the RHS of Eq. (44), we have a familiar "resistances in series" form for Kirchoff's Law in linear electric circuits. The numerator defines the reciprocal overall mass transfer coefficient for the two film transport problem for species U and the denominator for species V (see Eq. (8.5) of Bailey and

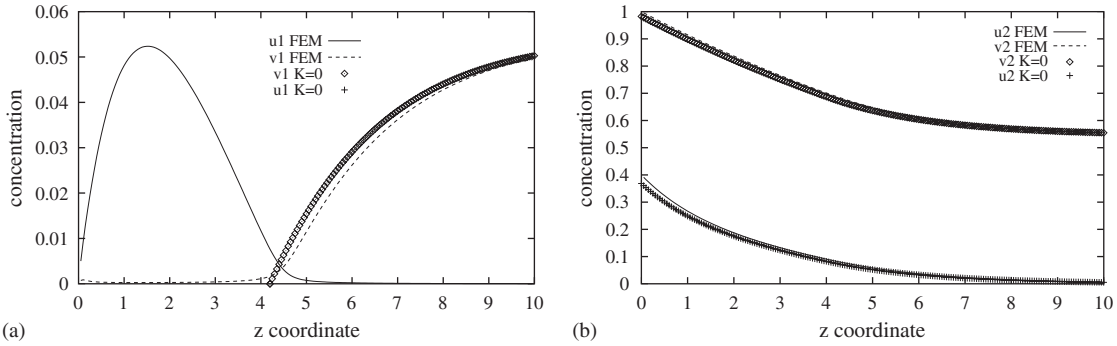

Fig. 4. (a) Reagent concentrations in phase I predicted by the irreversible theory ($K = 0$) and by the finite-element model (FEM) for fast, nearly irreversible kinetics. (b) Reagent concentration in the nonreactive phase II for the same models. Inlet values are $u_0 = 0.4$, $v_0 = 1.0$, and $h_U = 1$, $h_V = 0.1$, $h_W = 0.01$ and all mass transfer coefficient ratios $v_{u1} = v_{u2} = v_{v2}$ are unity, Peclet number $p = 5$ and for the FEM model, $K = 10^{-4}$ and $\varepsilon = 10^{-4}$. The crossover point, $X = 4.19$ is clearly discernible in the reacting phase concentrations.

Ollis (1987)). The meaning here is that only if the stoichiometric ratio is sufficiently skewed *away from* the more "volatile" component can crossover occur, and the meaning of such skewed stoichiometry follows from the combined times for mass transfer across both sides of the interface, weighted by the Henry's Law coefficient, so that total effective transfer time is faster for U (numerator) than for V (denominator). Furthermore, for crossover to exist, the condition $u_0 < v_0$ must hold.

3.5. Parametric study of the crossover length

In this subsection, we combine the parametric study of the crossover length from the finite Peclet number theory, computed from Eq. (38) and the full finite-element solution of the boundary value problem (11)–(17). The numerical algorithm only differs conceptually from that of Mchedlov-Petrossyan et al. (2003b) and that presented in Zimmerman et al. (2003) by doubling the number of differential and algebraic equations solved. The coding was analogous and the solutions to the 1-D stationary nonlinear DAEs were found by Galerkin finite-element methods on Lagrange quadratic elements on a 1000 element mesh of the interval $0 < z < 10$, with mesh independence validated by doubling the mesh resolution. The algebraic constraints were treated by the Newton–Raphson method, converging in eight iterations to 10^{-6} precision.

These solutions are reported as "FEM" in the legends of the following figures. The good agreement for a range of parameters with $K \ll 1$ serves as mutual validation for the fidelity of the theory and of the computational model.

Fig. 4 shows the bulk phase concentrations of the reactants approximated by the irreversible, fast reaction asymptotic theory and also the finite-element solution to the full governing equations (11)–(17) with nearly irreversible reaction. The agreement is good, but the error between computed values and the theory is visually discernible, even for $\varepsilon = 10^{-4}$ and $K = 10^{-4}$, and thus requires discussion. The finite-element solution was grid resolved on a grid scale of 100 elements per unit dimensionless length and verified by a 200 elements per unit refined mesh. The modest discrepancies between the computed profiles and the theory in Fig. 4(a) indicate that error is cumulative along the whole domain, typically due to stronger interaction between nonlinearity and diffusion than would be expected by formal scaling arguments. The gross features of the theory are borne out nonetheless, with crossover achieved in the reactive phase concentrations and its position and regions of near depletion of each reactant validated.

Although not shown, we also coded the finite-element solution to the unapproximated irreversible equations (18) and (19) with BCs and constraints given in Eqs. (14)–(17). These were visually superimposable with the FEM solution for $\varepsilon = 10^{-4}$, $K = 10^{-4}$. This additional information confirms our hypothesis that the formal error estimates of the perturbation theory do not hold uniformly. In particular, the estimates near the crossover point might improve with a distinctly different scaling. Our previous analysis of the batch reactor with dispersed phase dynamics (Mchedlov-Petrossyan et al., 2003a) and the nonequilibrium effects of finite-rate fast reaction (Zimmerman et al., 2005) used three regions—blowing up the coordinate in the vicinity of the switch time. Although such a methodology is plausible here, the theory put forth is self-consistent, leads to useful engineering predictions, and is analytically tractable.

Fig. 5 shows the largest discrepancy between the approximate theory for fast irreversible reaction and the full finite-element calculations. At small Peclet numbers, the theory substantially underpredicts the crossover point X. Strong diffusion couples with nonlinearity to migrate the crossover point downstream compared to the piecewise linear perturbation theory. Since high Peclet number operation is the norm, even with microscale flows, this discrepancy is not an overly limiting constraint on the applicability of the theory. Fifty parametric values of p were taken to form the FEM curve.

Fig. 6 shows good agreement for a modest Peclet number $p = 5$ for the predicted crossover point X from the perturbation theory and for the numerics while varying the stoichiometric ratio S. Again, the theory underpredicts the simulations, but the gap diminishes between the prediction and computed value for S approaching S_{crit}, i.e. longer pre-crossover regions. Fifty parametric values of S were taken to form the FEM curve in Fig. 6.

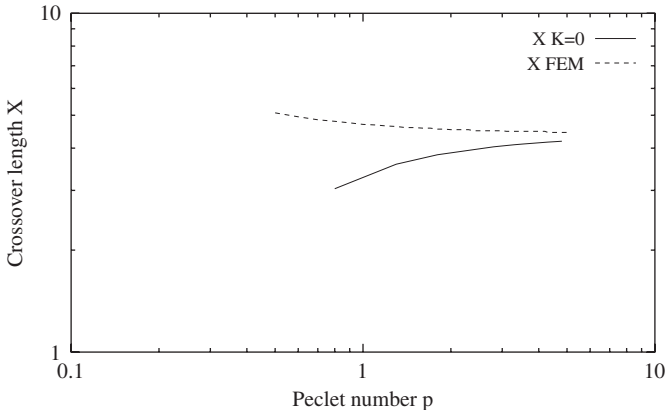

Fig. 5. Crossover point X vs. Peclet number p where inlet values are u_0=0.4, 1.0, with unit mass transfer ratios and $h_U = 1$, $h_V = 0.1$ with *irreversible*, *fast* reaction kinetics. Low peclet number, equivalent to dominant diffusion, causes the crossover point to recede to the origin. Strong convection results in the crossover point moving toward infinity. The graph also shows the FEM solution (parameters as in Fig. 2), which converges to the irreversible theory solution for high peclet number.

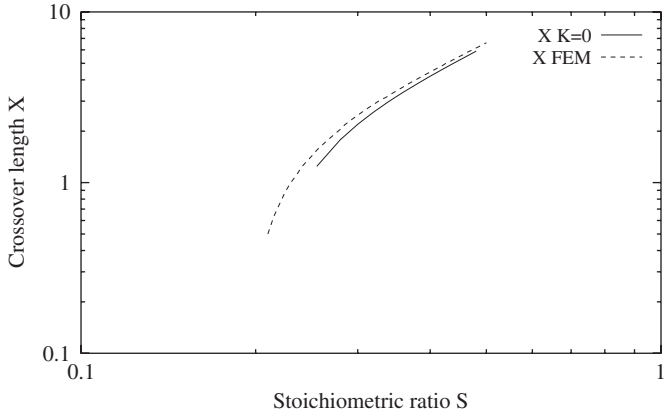

Fig. 6. Crossover point X vs. stoichiometric ratio $\sigma = u_0/v_0$ where $p = 5$, with unit mass transfer ratios and $h_U = 1$, $h_V = 0.1$, with *irreversible*, *fast* reaction kinetics.

Fig. 7 shows the good agreement for a modest Peclet number $p = 5$ for crossover point X between the theory and numerics for variation of the partition coefficient h_V. Here, the best agreement is as $h_V \to 0$, and the theory still underpredicts the numerics slightly. Fifty parametric values of h_V were taken to form the FEM curve. The underlying message from all these parametric studies is that crossover is a well-predicted phenomenon in all cases shown, i.e. the infinite Peclet number bounds on $S_{\text{crit}}(h)$ and $h_{\text{crit}}(S)$, Eq. (43), used to determine the range of the numerical parametric study are a faithful indicator of the existence of crossover. Thus, the claim that the infinite p limit provides a design boundary on crossover is supported. Conservatively, if h and S are within the critical curve defined by Eq. (43), or equivalently in the hyperspace bounded by Eq. (44), then the full numerical solution to Eqs. (11)–(17) indicates that crossover will occur, regardless of the Peclet number. This parametric map for the solution structure is well supported by

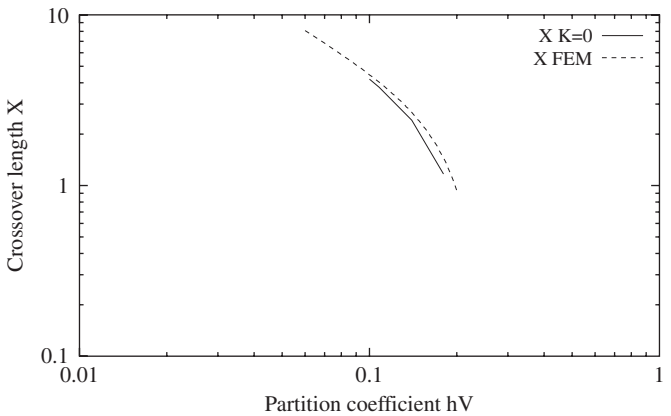

Fig. 7. Crossover point X vs. partition coefficient h_V at fixed $p_U = 1$ for p=5 with S=0.4, and unit mass transfer ratios with *irreversible*, *fast* reaction kinetics.

the numerics. Subordinately, the detail of the crossover length predicted holds exceedingly well for all but low Peclet numbers, where nonlinearity, especially in the vicinity of the crossover point, is stronger than expected by naive scaling arguments underpinning our perturbation analysis.

3.6. Reactor efficiency

In this section, we explore the engineering utility of crossover. The argument in our past works for a dispersed reacting phase was that crossover led to localization of intensified reaction in the vicinity of the crossover point. Crossover sets the scale (time for batch reactors) of the 99% fractional conversion and thus optimizing the crossover point with regard to reactor efficiency optimizes the global performance. Furthermore, that localization leads to intensification was also shown to lead to efficiency. The 99% fractional conversion time was much shorter when crossover occurs in batch reactors, and the length much shorter for premixed tubular reactors, than in absence of crossover with the same stoichiometric excess. This is easily explained by the combined effects of reaction and separation driving the equilibrium when crossover occurs. It is not at all apparent a priori that crossover gives an efficiency boost similar to reactive separation, nor should be classed as reactive separation. We show in this section that localization from crossover does lead to intensification and thus enhanced efficiency.

3.6.1. Numerical analysis of reactor efficiency

Fig. 8(a) shows the results of the numerical analysis of the full model equations for the product in the reacting phase, which shows greatest production in the interval surrounding the crossover length. The build up of W in the nonreacting phase follows from its relative rejection from the reacting phase, due to phase equilibrium, $h_W = 0.01$. It is clear that at $z = 10$, the reaction is essentially complete with $v_0 - u_0 \approx w_1 + w_2$. The localization illustrated in product formation in the reacting phase is in accord with the notion that the precrossover region

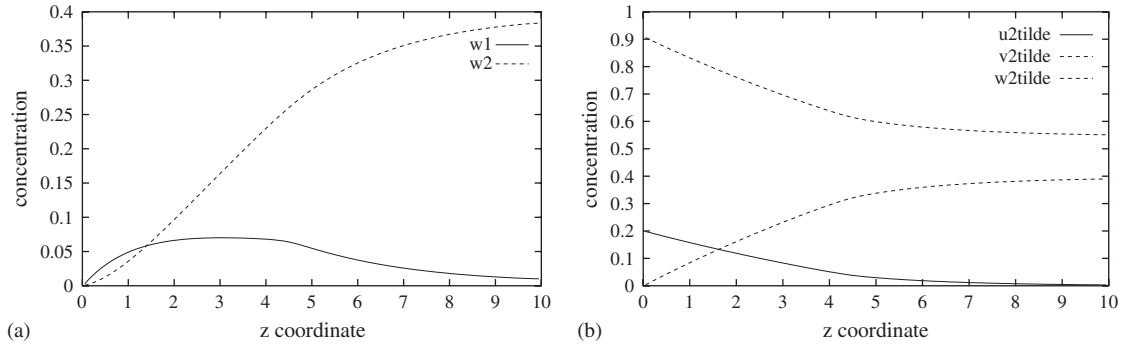

Fig. 8. (a) Product concentrations in both phases predicted by the finite element model (FEM) for fast, nearly irreversible kinetics. (b) Interfacial concentrations $(\tilde{u}_1, \tilde{v}_1, \tilde{w}_1)$ in the reactive phase I for the same model. Inlet values are $u_0 = 0.4$, $v_0 = 1.0$, and $h_U = 1$, $h_V = 0.1$, $h_W = 0.01$ and all mass transfer coefficient ratios $v_{u1} = v_{u2} = v_{v2}$ are unity, Peclet number $p = 5$ and for the FEM model, $K = 10^{-4}$ and $\varepsilon = 10^{-4}$.

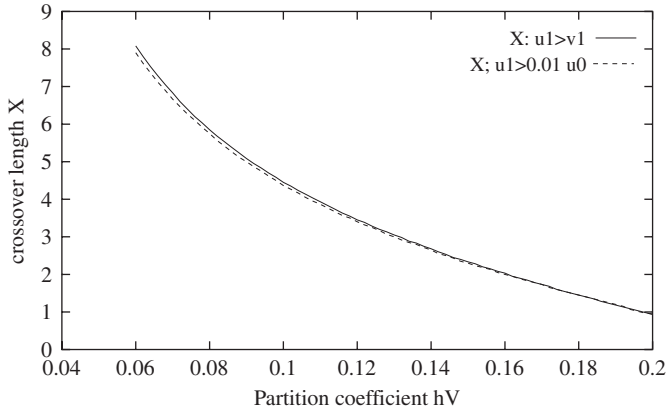

Fig. 9. Two notions for the crossover length computed for the FEM model: (1) crossover when $u_1 = v_1$; (2) crossover when $u_1 = 0.01u_0$ for varying partition coefficient h_V with fixed $p = 5$, $S = 0.4$, and $h_U = 1$ computed from FEM model with $K = 10^{-4}$ and $\varepsilon = 10^{-4}$ and $h_W = 0.01$.

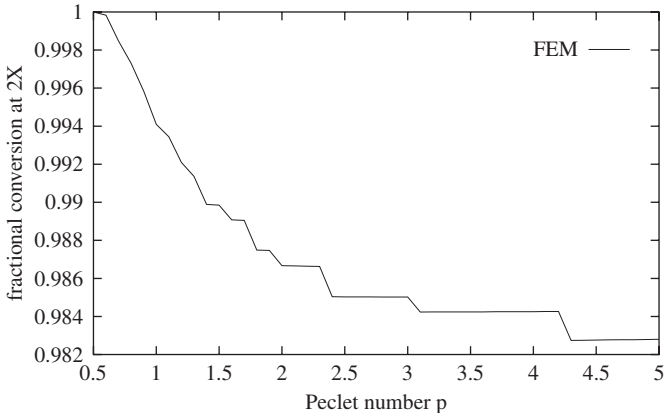

Fig. 10. Fractional conversion at the crossover point X for varying Peclet number p with $S = 0.4$, $h_U = 1$, $h_V = 0.1$ computed from the fast, irreversible theory.

has the greatest usage efficiency in reacting the stoichiometrically limiting reactant. Fig. 8(b) is included for completeness. The profiles of interfacial concentrations (shown here in phase II, but those in phase I are slaved to these by the Henry's Law relations) show the expected qualitative behavior—$\tilde{u}_2$ is exhausted by reaction, $\tilde{v}_2$ is diminished downstream, and $\tilde{w}_2$ rises towards the value indicated by the initial u_0 charge being consumed completely. The major qualitative result from this figure is the localization—nearly all variation occurs prior to X, with only some modest modification due to postcrossover dynamics.

Fig. 9 introduces two numerical estimates of the crossover point:

$$X_{u_1>v_1} = \int_\Omega (u_1 > v_1)\, \mathrm{d}\Omega,$$

$$X_{99\%} = \int_\Omega (u_1 > 0.01u_0)\, \mathrm{d}\Omega. \tag{45}$$

The use of logical operation is a convenience for interpolating within the finite-element functional representation of the numerical solution. These definitions are construed as "crossover when the reactants have identical concentration in the reacting phase" and "crossover when the limiting reactant is nearly exhausted in the reacting phase." These definitions are clearly sufficiently close to each other in value to be interchangeable in utility. In the subsequent analysis, we have used $X_{u_1>v_1}$ and simply refer to it as the crossover point.

First we consider the full numerical simulations of Eqs. (11)–(17). At low Peclet numbers, $p \in [0.5, 5]$ shown, the region of size twice the crossover length contains between 98% and 100% of the fractional conversion, according to Fig. 10. Although this localization is diminished somewhat with increasing Peclet number, the high degree of localization indicates that reaction is more intense in the vicinity of the crossover point. This is not unexpected as the crossover point has the greatest molecular efficiency since both reactants react nearly instantaneously at crossover as they arrive in the reacting phase.

Fig. 11 shows that the approach to the limiting S, S_{crit}, for the infinite Peclet number theory (43) leads to most intense fractional conversion in the region $[0, 2X]$. Interestingly, this is also the regime for the greatest fidelity between the irreversible theory and the numerics. Fig. 12 explores the same question of localization with regard to variation of the partition coefficient h_V. Here, smaller h_V leads to greater "volatility," maximizing

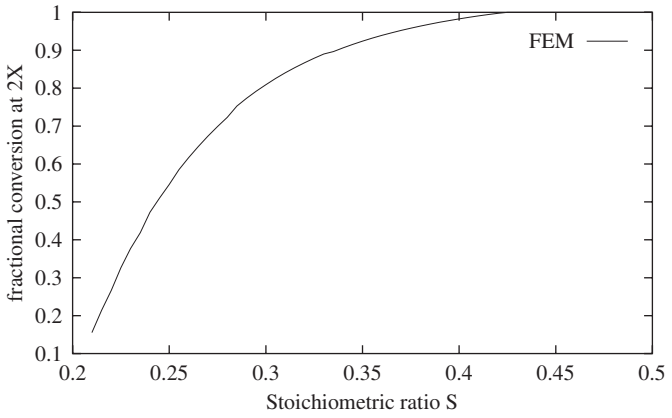

Fig. 11. Fractional conversion at the crossover point X for varying stoichiometric ratio S with fixed $p=5$, $h_U=1$, $h_V=0.1$ computed from the fast, irreversible theory.

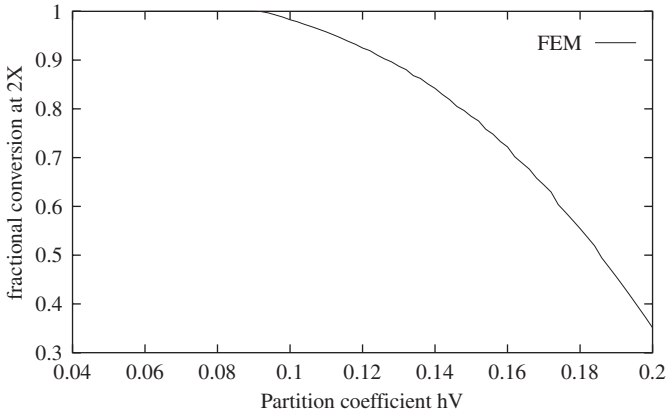

Fig. 12. Fractional conversion at the crossover point X for varying partition coefficient h_V with fixed $p=5$, $S=0.4$, and $h_U=1$ computed from the fast, irreversible theory.

the fractional conversion. This is intuitive, and is in accord with our original motivation for this study. Up to this point, X refers to the inferred X from the numerics.

3.6.2. Fractional conversion from the irreversible theory

Even though the dynamics of the product decouple from the reactants in the irreversible limit, the irreversible theory can be used to predict the fractional conversion at any position by recognizing that the disappearance from the nonreacting phase of U equates to the formation of W. Thus, for instance, when $u_2^{(0)}=0.01u_0$, 99% conversion is achieved. Using the analytic solution, this position $z=z_{99}$ can be computed by root finding algorithms. Furthermore, a broader range of parameters can be easily treated without redefining computational domain and mesh as needed for numerical analysis in the previous subsection.

Fig. 13 reports the ratio z_{99}/X with variation of Peclet number on a log–linear scale. Clearly, there is little localization in the fractional conversion for $p<1$. For high p there is a plateau which is approached even at $p\sim 5$ with this ratio slowly

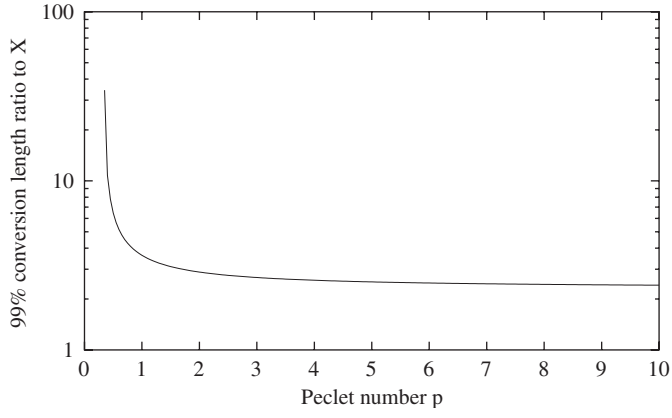

Fig. 13. Ratio of the 99% conversion length to the crossover length X for varying Peclet number p with $S=0.4$, $h_U=1$, $h_V=0.1$ computed from the fast, irreversible theory.

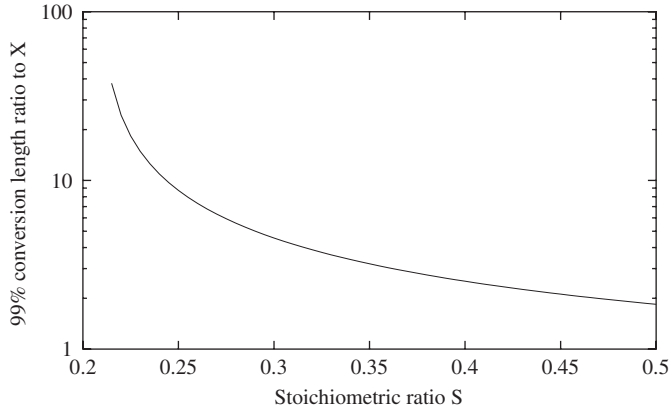

Fig. 14. Ratio of the 99% conversion length to the crossover length X for varying stoichiometric ration S with fixed $p=5$, $h_U=1$, $h_V=0.1$ computed from the fast, irreversible theory.

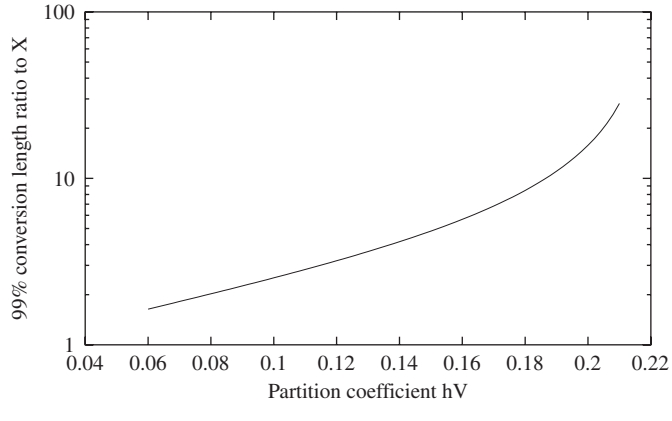

Fig. 15. Ratio of the 99% conversion length to the crossover length X for varying partition coefficient h_V with fixed $p=5$, $S=0.4$, and $h_U=1$ computed from the fast, irreversible theory.

decaying from $z_{99}/X\sim 2.4$. This indicates that the 99% conversion level is set by the crossover length scale, and Fig. 10 corroborates this assertion.

Fig. 14 answers the same question posed for the stoichiometric (deficit) ratio S. Although the curve has not flattened as

$S \to S_{\text{crit}}$, it does achieve its minimum value ($z_{99}/X < 2$) in this limit. This feature of most localized conversion as $S \to S_{\text{crit}}$ is corroborated numerically by Fig. 11.

Fig. 15 parallels Fig. 12 in showing variation with h_V of a measure of localization. The conclusion is that $h_v \to h_{V,\text{crit}}(S)$ gives the worst localization, and $h_V \to 0$ gives the best.

4. Conclusions

Here a representative configuration for two-phase reactive extraction with two-layer flow, applicable in a microfluidic device, is analyzed for the occurrence of crossover. Analogous to the integration of reaction and separation, crossover can be exploited to enhance irreversible reactions in the direction of the desired product using multiphase flow contacting. In the case of nearly irreversible, fast reactions, however, the dynamics of the product have little influence on the reactor efficiency in say liquid–liquid reactive extraction. A similar intensification in reaction efficiency to reactive separation can be achieved by exploiting phase equilibrium or asymmetry in mass transfer rates of the reactants. Here, a model for two-layer biphasic flow and homogeneous reaction is proposed for co-current reactive extraction, demonstrating that localization and intensification of reaction occurs in the region between the entrance and crossover. Crossover occurs if the reactant in stoichiometric deficit preferentially populates the reacting phase due to sufficient imbalance in either mass transfer coefficients or phase equilibrium. We develop an infinite Peclet number (convection dominates over bulk diffusion) model that indicates that crossover occurs when

$$1 > \frac{u_0}{v_0} > \frac{\dfrac{1}{\kappa_{u2}} + \dfrac{1}{\kappa_{u1} h_U}}{\dfrac{1}{\kappa_{v2}} + \dfrac{1}{\kappa_{v1} h_V}}$$

for fast, irreversible reactions. u_0 and v_0 are initial charges to the tubular reactor, the κ's are mass transfer coefficients for each side of the fluid interface and the h's are Henry's Law coefficients for reactants U and V. The interpretation of this formula is that if $v_0 > u_0$, then crossover will occur if the overall mass transfer rate of U is faster than the overall mass transfer rate for V. Downstream of the crossover point, the reactant in stoichiometric excess also dominates the reacting phase due to relative exhaustion of the more mobile component. A finite Peclet number theory for fast, irreversible reaction shows that the above formula is a conservative limit for crossover—if it holds, crossover will occur regardless of the Peclet number. A formula for the larger parametric region for crossover with finite Peclet number is derived. Verification that crossover is achieved is found by finite-element numerical analysis of the full governing equations. Both theory and numerical analysis predict localization and intensification of the reaction due to crossover. Crossover sets the length scale as approximately two and a half crossover lengths for completed reaction for sufficiently high Peclet number with strong kinetic asymmetry. The theory predicts that taking the ratio of inlet concentrations $S = u_0/v_0$ to be the critical value at fixed physical parameters for mass transfer and phase equilibrium maximizes localization and reactor efficiency. Similarly, the kinetic asymmetry should be as large as possible to exploit the benefits of crossover.

Acknowledgments

GAK and WBZ thank the French–British Program Egide for their research grant. WBZ would like to thank the Universite du Littoral for a visiting professorship, the EPSRC Advanced Research Fellowship Programme, and the Royal Academy of Engineering/Leverhulme Trust for a Senior Research Fellowship. WBZ and GAK thank the British Council Alliance Programme for a travel award, PN02.061. POMP would like to thank the University du Littoral Côte d'Opale, France, for a visiting Professorship and Région Nord Pas de Calais for a research fellowship. WZ acknowledges support under EPSRC grant nos. GR/R72754, GR/A01435, and GR/S83746.

References

Bailey, J.E., Ollis, D.F., 1987. Biochemical Engineering Fundamentals. Chemical Engineering Series. McGraw-Hill, New York, p. 464.

Bart, H.J., 2003. Reactive extraction in stirred columns—A review. Chemical Engineering and Technology 26 (7), 723–731.

Bischoff, K.B., 1961. A note on boundary conditions for flow reactors. Chemical Engineering Science 16, 131.

Danckwerts, P.V., 1953. Continuous flow systems. Distribution of residence times. Chemical Engineering Science 2, 1–18.

Deshpande, K.B., Zimmerman, W.B., 2005a. Experimental study of mass transfer limited reaction. Part I: a novel approach to infer asymmetric mass transfer coefficients. Chemical Engineering Science 60 (11), 2879–2893.

Deshpande, K.B., Zimmerman, W.B., 2005b. Experimental study of mass transfer limited reaction. Part II: existence of crossover phenomenon. Chemical Engineering Science 60 (15), 4147–4156.

Deshpande, K.B., Zimmerman, W.B., 2006a. Simulation of droplet dynamics and interfacial mass transfer using the level set method. Chemical Engineering Science 61 (19), 6486–6498.

Deshpande, K.B., Zimmerman, W.B., 2006b. Simulation of mass transfer limited reaction in a moving droplet. Chemical Engineering Science 61 (19), 6424–6441.

Fogler, H.S., 1992. Elements of chemical reaction engineering. In: Amundson, N. (Ed.), Series in the Physical and Chemical Engineering Sciences. Prentice-Hall, Englewood Cliffs, NJ, p. 241ff.

Gorak, A., 2003. Special issue on reactive separations. Chemical Engineering and Processing 42 (3), 135.

Hill, C.G., 1977. An Introduction to Chemical Engineering Kinetics and Reactor Design. Wiley, New York.

Krishna, R., 2002. Reactive separations: more ways to skin a cat. Chemical Engineering Science 57 (9), 1491–1504.

Lazarova, Z., Syska, B., Schugerl, K., 2002. Application of large-scale hollow fiber membrane contactors for simultaneous extractive removal and stripping of penicillin G. Journal of Membrane Science 202 (1–2), 151–164.

Levenspiel, O., 1972. Chemical Reaction Engineering. second ed. Wiley, New York.

Mchedlov-Petrossyan, P.O., Zimmerman, W.B., Khomenko, G.A., 2003a. Fast binary reactions in a heterogeneous catalytic batch reactor. Chemical Engineering Science 58/12, 2691–2703.

Mchedlov-Petrossyan, P., Khomenko, G., Zimmerman, W.B., 2003b. Nearly irreversible, fast heterogeneous reactions in premixed flow. Chemical Engineering Science 58/13, 3005–3023.

Prat, L., Guiraud, P., Rigal, L., Gourdon, C., 2002. A one dimensional model for the prediction of extraction yields in a two phases modified twin-screw extruder. Chemical Engineering and Processing 41 (9), 743–751.

Pursell, M.R., Mendes–Tatsis, M.A., Stuckey, D.C., 2003a. Co-extraction during reactive extraction of phenylalanine using Aliquat 336: interfacial mass transfer. Biotechnological Progress 19 (2), 469–476.

Pursell, M.R., Mendes-Tatsis, M.A., Stuckey, D.C., 2003b. Co-extraction during reactive extraction of phenylalanine using Aliquat 336: modeling extraction equilibrium. Biotechology and Bioengineering 82 (5), 533–542.

Schembecker, G., Tlatlik, S., 2003. Process synthesis for reactive separations. Chemical Engineering and Technology 42 (3), 179–189.

Song, H., Tice, J.D., Ismagilov, R.F., 2003. A microfluidic system for controlling reaction networks in time. Angewandte Chemie-International Edition 42 (7), 768–772.

Zimmerman, W.B., Mchedlov-Petrossyan, P.O., Khomenko, G.A., 2003. Transport Limited Heterogeneous Catalysis. World Scientific, Singapore, in preparation, see ⟨http://eyrie.shef.ac.uk/will/heteroca⟩.

Zimmerman, W.B., Mchedlov-Petrossyan, P., Khomenko, G.A., 2005. Nonequilibrium effects on fast binary reactions in a heterogeneous catalytic batch reactor. Chemical Engineering Science 60, 3061–3076.

Further Reading

Cutlip, M.B., Shacham, M., 1999. Problem Solving in Chemical Engineering with Numerical Methods. Prentice-Hall, Upper Saddle River, NJ.

Mchedlov-Petrossyan, P.O., 1998. Heterogeneous diffusion-limited chemical reactions of initially segregated species. Kharkov University Bulletin, Chemistry Series 2, 97–101.

Mills, P.L., Chaudhari, R.V., 1997. Multiphase catalytic reactor engineering and design for pharmaceuticals and fine chemicals. Catalysis Today 37 (4), 367–404.

Zimmerman, W.B., Mchedlov-Petrossyan, P.O., Khomenko, G.A., 1999. Diffusion limited mixing and reaction in heterogeneous catalysis of initially segregated species. IChemE Symposium Series 146, 317–324.

Zimmerman, W.B., 2004. Process Modeling and Simulation with Finite Element Methods. Series A on Stability, Vibration and Control of Systems, vol. 15, World Scientific, Singapore.